Shifts in electron capture to the continuum at low collision energies: Enhanced role of target postcollision interactions

M. B. Shah,[1] C. McGrath,[1] Clara Illescas,[2] B. Pons,[2,3] A. Riera,[2] H. Luna,[1] D. S. F. Crothers,[1] S. F. C. O'Rourke,[1] and H. B. Gilbody[1]

[1]*Department of Pure and Applied Physics, School of Mathematics and Physics, Queen's University of Belfast, Belfast BT7 1NN, United Kingdom*

[2]*Laboratorio de Física Atómica y Molecular en Plasmas de Fusión Nuclear, Asociado al Laboratorio Nacional de Fusión por Confinamiento Magnético del CIEMAT, Departamento de Química C-IX, Universidad Autónoma de Madrid, Cantoblanco, 28049 Madrid, Spain*

[3]*Centre Lasers Intenses et Applications, UMR 5107 du CNRS, Université de Bordeaux-I, 351 Cours de la Libération, F-33405 Talence, France*

Measurements of electron velocity distributions emitted at $0°$ for collisions of 10- and 20-keV H^+ incident ions on H_2 and He show that the electron capture to the continuum cusp formation, which is still possible at these low impact energies, is shifted to lower momenta than its standard position (centered on the projectile velocity), as recently predicted. Classical trajectory Monte Carlo calculations reproduce the observations remarkably well, and indicate that a long-range residual interaction of the electron with the target ion after ionization is responsible for the shifts, which is a general effect that is enhanced at low nuclear velocities.

One of the most striking features of ionization processes in ion-atom collisions is the cusplike peak that appears in the spectrum of emitted electrons when the velocity of the electron, $\mathbf{v}_e$, matches that of the projectile, $\mathbf{v}$. This phenomenon is called "electron capture to the continuum" (ECC), following the heuristic interpretation of early measurements [1–3], in terms of electrons being "captured" in continuum states of the projectile [4]. Those cusp electrons have received a great deal of attention from both experimental [5–10] and theoretical [11–17] sides. Most of the experiments have been performed in the intermediate- and high-energy ranges using electron spectroscopy, where the electron spectrum is scanned in energy and angle (see, e.g., Refs. [1–3,5–8]), and specific traces of cusp electron formation have also been identified in recoil-ion momentum distributions, by means of the COLTRIMS technique [9,10].

From the theoretical side, it was soon realized [11,12] that the description of the ECC process is beyond single-center theoretical treatments; perturbative models were thus derived [11–17], with particular allowance for the distortion of the inital and/or final wave functions by both the target and projectile Coulomb fields. Furthermore, a partial confirmation of the heuristic explanation was obtained from classical trajectory Monte Carlo (CTMC) calculations [18,19], which allow a direct following of the mechanism. In this context, Reinhold and Olson [18] showed how electron-projectile interactions play an essential role in the formation of the cusp until very large internuclear distances, while electron-target ones induce its asymmetry. Similarly, CTMC calculations for p+He collisions using an improved initial condition [20], carried out in a joint theoretical-experimental endeavour [21], concluded that the ECC electrons are first captured in Rydberg states of the projectile with energies with respect to this nucleus close to zero, and then become ionized; after ionization, the energy is approximately conserved. Two new features were also explained in Ref. [20]: (i) that the ECC cusp

is indeed a cusp, and not a divergence smoothed by the experiment; and (ii) that its peak value is not situated at exactly the projectile velocity, as usually assumed [4,11,12].

Obviously, a definite statement on these two points requires an experimental confirmation, and in the present work we focus on the second feature. In Ref. [20], we reported a preliminary confirmation of the theoretical findings by comparing probabilities for a single nuclear trajectory with raw experimental data. Here we aim at more definite conclusions, by comparing calculated double differential cross sections to the data from a specially designed, state-of-the-art set-up to measure the shift of the ECC peak at small impact energies for which the effect is enhanced. As benchmarks we have chosen 10- and 20-keV H^++He and H^++H_2 collisions.

It should be emphasized that accurate observations (for the present purpose) of low-energy electrons at $0°$ are a difficult task. A major problem arises through the small amount of gas spillage into the electron energy analyzer and the surrounding regions when target gas is introduced into the system. The projectile beam, in transit through the analyzer, can make ionizing collisions with the spilled gas and produce spurious electrons that can completely mask the yield of electrons from the process under study [22]. However, our recent triple differentially pumped target geometry [8] has succeeded in considerably reducing this gas spillage, thereby dramatically reducing this background contribution and allowing us to measure the velocity distributions with unprecedented resolution over a very large velocity range including the difficult region of almost zero velocities.

Our measurements were carried out using a large hemispherical analyzer spectrometer capable of measuring electrons emitted at $0°$ with energies down to 2 eV. Thus, even at an impact energy of 10 keV, electrons with velocities well below the ECC cusp can be detected. No electrostatic lens system is used to collect the electrons. Electrons are instead allowed to simply drift into the spectrometer so only those
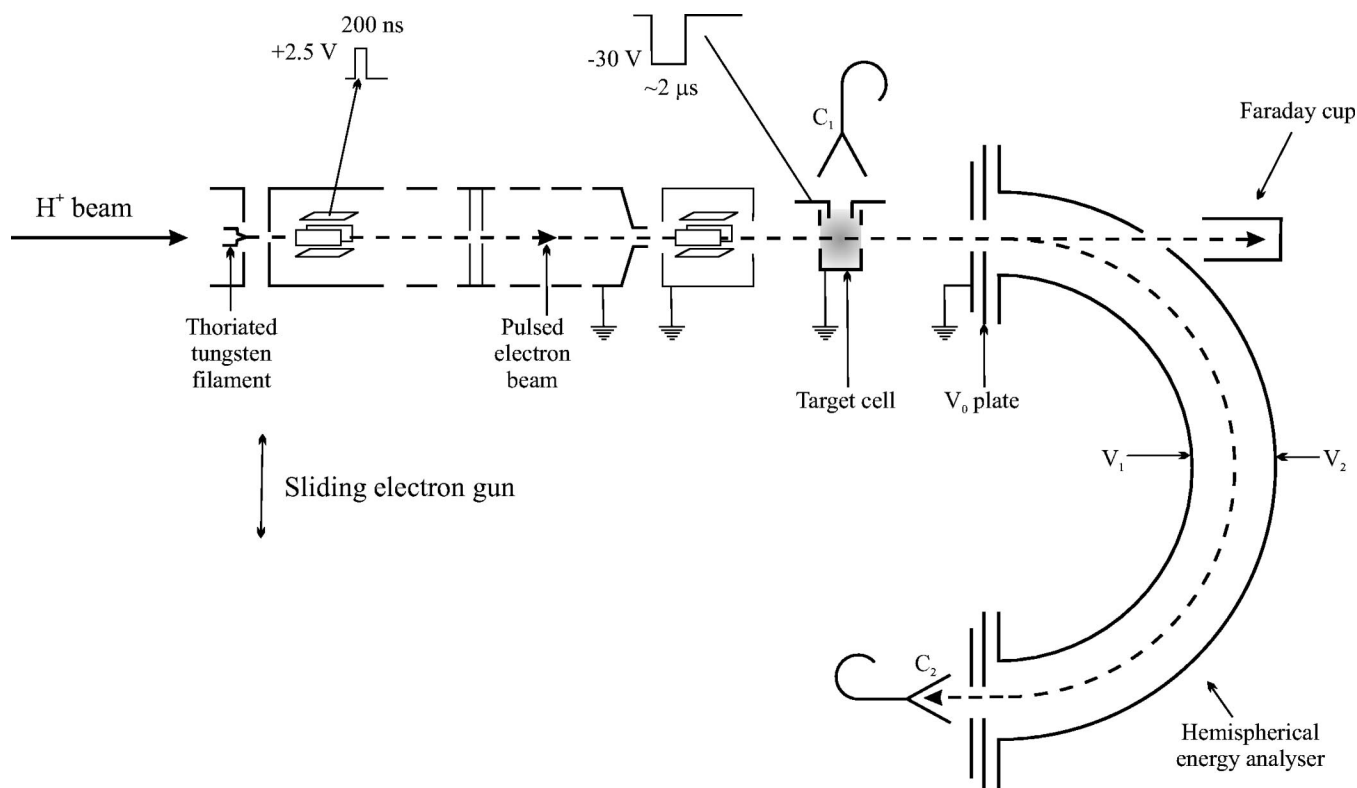
FIG. 1. Schematic diagram of the experimental setup designed to detect $0°$ electron emission in low-energy collisions.

emitted with initial directions at $0°$ are recorded. The apparatus is fully described in our recent paper [8] and only a brief description will be given here together with a fuller description of the modification that were specifically incorporated for the present low-energy measurements. The apparatus highlighting the present modifications is shown in Fig. 1. The reader is referred to Ref. [8] for details on the hemispherical energy analyzer spectrometer, target gas geometry, and the triple differential pumping arrangement.

A beam of H^+ ions passes through the target cell and enters the large hemispherical analyzer spectrometer (together with electrons emitted at $0°$ from the target) before being collected in a Faraday cup. The electrons travel through a 50-mm drift region before entering the spectrometer. The acceptance angle of the spectrometer is $1.5°$ while the energy resolution $\Delta E/E$ is 0.012 (full width at half maximum). The spectrometer was operated at the pass energy of 7 eV. The spectrometer, the target cell, and the surrounding region are carefully screened from the Earth's magnetic field by a double layer of 2-mm-thick mu-metal sheets.

The electron distribution was recorded with the gas introduced into the target cell and this was then carefully corrected by subtracting the corresponding distribution obtained when the main chamber was flooded with gas to a pressure equal to the value attained when gas was introduced in the target cell.

For the purpose of calibrating the spectrometer, we use electrons obtained from a sliding electron gun pushed in the path of the ion beam, to pass through the spectrometer. Since the energy of the electrons emanating from the gun is not precisely known, the energy is assigned to the electron beam

by use of the threshold ionization technique. For this purpose, the electron gun is operated in a pulsed beam mode [23]. Electron beam pulses of 200-ns duration at a repetition rate of 5×104 pulses/s collide with the target gas before entering the spectrometer where their energies are determined simultaneously. Target product ions formed through collisions with the electron beam are collected by a delayed extraction pulse applied across the target cell and detected by the channeltron $C1$. A time-of-flight technique [23] is used to identify and record the product ions. For the H_2 target, the plot in Fig. 2 shows that a voltage of 14.8 V applied to the tip of the tungsten filament of the electron gun corresponds to the threshold energy of 15.4 eV for the ionization of H_2.

When an electron beam defined in this way is analyzed by the spectrometer, the voltages applied to the inner and the outer hemispheres of the spectrometer are found to be in very good agreement with the values calculated from the standard formula given by Kuyatt and Simpson [24]. Perhaps this is not surprising since a layer of graphite covers the inside surfaces of the target cell and the spectrometer. The $0°$ electrons, therefore, see the same material from their moment of origin to the final moment of their detection and do not encounter changes in the contact potentials along their journey. This study confirms that our spectrometer is functioning correctly and any changes we observe in the velocity distributions of the $0°$ electrons must be genuine.

Turning now to our theoretical calculations, we have treated the interaction of the "active" electron with the He^+ and H_2^+ cores in terms of an effective potential Z_{eff}/r, with $Z_{eff} = 1.6875$ and 1.099 45, respectively. We have calculated
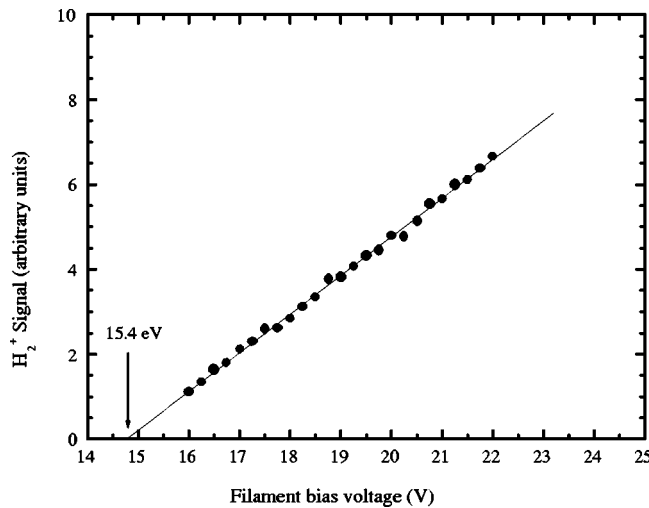
FIG. 2. Variation of the H_2^+ signal as a function of the voltage applied to the tip of the tungsten filament (see Fig. 1).

the cross sections with impact-parameter CTMC treatments [25], whose initial distributions were taken to be superpositions of ten microcanonical ensembles that were constucted as in Ref. [26] to yield a good fit to the quantal momentum and spatial densities for the lowest eigenstate of the corresponding model Hamiltonian; this is a crucial step to achieve agreement with COLTRIMS data.

The Hamilton equations were then integrated for an ensemble of $N=2.5\times10^6$ sample electrons per nuclear trajec-

tory in the case of 10-keV collisions ($N=2\times10^6$ for 20 keV). The ECC electrons were selected by means of the usual energy criterion at an integration time of 2×10^6 a.u., together with an angular selection $\Delta\theta\leqslant1.5°$ about the projectile direction to match the experiment. Doubly differential cross sections (DDCS) for single ionization were obtained in the frame of the independent-particle model [27] according to

$$\frac{d\sigma}{d\Omega\,dp}(\theta,p)=\frac{4\pi\Delta b}{\Delta\Omega\Delta p}\sum_k b_k P_e(b_k)\frac{n(b_k)}{N},\qquad(1)$$

where $n(b_k)$ is the number of ionized electrons collected in the solid angle of aperture $\Delta\Omega$ centered on $\theta=0°$ and in the momentum interval $(p-\Delta p/2,p+\Delta p/2)$ along the nuclear trajectory with impact parameter b_k, P_e is the elastic probability, and Δb the impact parameter spacing.

Figure 3 shows our measured DDCS for electron emission at $0°$ for 10- and 20-keV protons in He and H_2, respectively. Since we are focusing on the (possible) shift in the ECC cusp, these data have been normalized to our classical results for the cross section.

The main conclusions from Fig. 3 are: (i) that an ECC cusp is formed at such low impact energies as at 10 and 20 keV, in both H_2 and He collisions; (ii) that these cusps peak at $v_e<v$; (iii) that experiment and theory agree remarkably well, except for the asymmetry on the left of the peak for the very small cross section for $p+He$ at 10 keV.
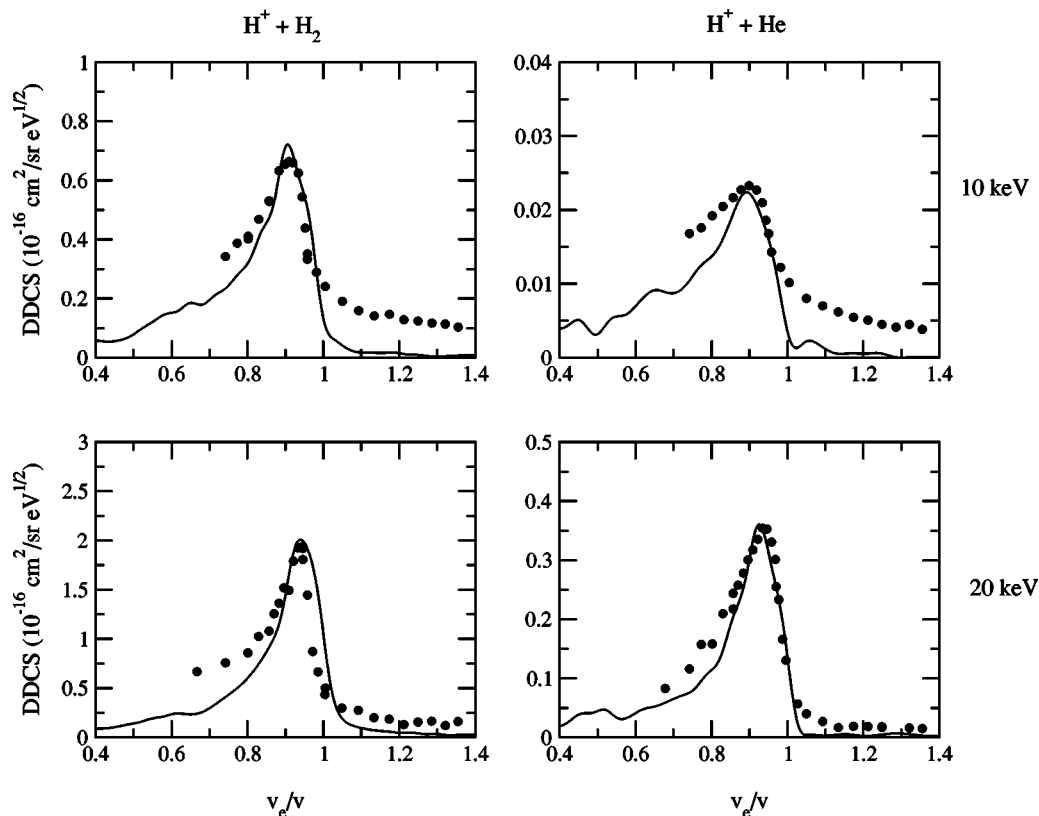
FIG. 3. DDCS for electron emission at $0°$ in 10- and 20-keV $p+He$, H_2 collisions: black points, present measurements; lines, CMTC calculations.

It should be noted that conclusion (iii) is not surprising once (i) and (ii) are confirmed. On one hand, the success of the improved CTMC method in describing the ionization mechanism, which relies on the adequacy of its statistical formulation and on the specific nature of the Coulomb interaction, has already been studied in Refs. [28,29]. On the other hand, the appropriateness of the additional approximations of the present treatment, i.e., the use of an independent particle model and of effective target potentials, follows from the particular mechanism under study, which implies (mono)electronic transitions occuring at large internuclear distances, where a simplified isotropic description is expected (and found) to be valid.

As shown in Ref. [20], both the shift and the asymmetry of the ECC cusp are postcollisional effects that follow from the pull of the target on the ionized electron after it becomes free, and are therefore clear outcomes of the so-called two-center effects [30]. This was proven by cancelling artificially the target-electron interactions at the time of ionization, whereby the cusp transforms into a peak at $\mathbf{v}_e = \mathbf{v}$. The pull from the target is obviously more effective for slower collisions, and so are the corresponding postcollisional effects. This is clearly confirmed by our measurements: as the impact energy decreases, the ECC cusp shifts towards lower velocities, and its width increases at both the low- and high-energy ends, in marked contrast to our previous high collision energy measurements [8,31] where the ECC cusps were shown to have a very sharp fall off.

To sum up, careful measurements of electron emission at $0°$ in low-energy $p + \mathrm{He}$, H_2 collisions have been reported. An unambiguous signature of the ECC process appears in the spectra, and the related cusp does not exactly peak at the projectile velocity. CTMC calculations nicely reproduce these experimental findings, and shed light on the nature of the shift, as stemming from the residual pull of the target on the ionized electrons after ionization, which is an effect that is enhanced at low nuclear velocities. By considering two impact energies and two collisional systems, we think that we can safely venture to state that the shift is a genuine and universal feature of the ECC phenomenon. Our explanation for the reason why it has not hitherto been described is that most previous measurements have been performed for energy ranges where the target postcollisional effects are weak.

[1] M.E. Rudd and T. Jorgensen, Jr., Phys. Rev. **131**, 666 (1963).

[2] M.E. Rudd, C.A. Sautter, and C.L. Bailey, Phys. Rev. **151**, 20 (1966).

[3] G.B. Crooks and M.E. Rudd, Phys. Rev. Lett. **25**, 1599 (1970).

[4] M. E. Rudd, private communication, cited in J. Macek, Phys. Rev. A **1**, 235 (1970); see also M.E. Rudd and J. Macek, Case Stud. At. Phys. **3**, 47 (1972).

[5] G. Bernardi, S. Suarez, P. Fainstein, C. Garibotti, W. Meckbach, and P. Focke, Phys. Rev. A **40**, 6863 (1989).

[6] D.H. Lee, P. Richard, T.J.M. Zouros, J.M. Sanders, J.L. Shinpaugh, and H. Hidmi, Phys. Rev. A **41**, 4816 (1990).

[7] L. Sarkadi, U. Brinkmann, A. Bader, R. Hippler, K. Tokesi, and L. Gulyas, Phys. Rev. A **58**, 296 (1998).

[8] C. McGrath, D.M. McSherry, M.B. Shah, S.F.C. O'Rourke, D.S.F. Crothers, G. Montegomery, H.B. Gilbody, C. Illescas, and A. Riera, J. Phys. B **33**, 3693 (2000).

[9] Th. Weber, Kh. Khayyat, R. Dorner, V.D. Rodriguez, V. Mergel, O. Jagutzki, L. Schmidt, K.A. Muller, F. Afaneh, A. Gonzalez, and A. Schmidt-Bocking, Phys. Rev. Lett. **86**, 224 (2001).

[10] L. An, Kh. Khayyat, and M. Schulz, Phys. Rev. A **63**, 030703 (2001).

[11] A. Salin, J. Phys. B **2**, 631 (1969); **5**, 979 (1972).

[12] J. Macek, Phys. Rev. A **1**, 235 (1970).

[13] Dz. Belkic, J. Phys. B **11**, 3529 (1978).

[14] D.S.F. Crothers and J.F. McCann, J. Phys. B **16**, 3229 (1983).

[15] P.D. Fainstein, V.H. Ponce, and R.D. Rivarola, J. Phys. B **24**, 3091 (1991).

[16] R.O. Barrachina, Nucl. Instrum. Methods Phys. Res. B **124**, 198 (1997).

[17] J. Fiol, R.O. Barrachina, and V.D. Rodriguez, J. Phys. B **35**, 149 (2002).

[18] C.O. Reinhold and R.E. Olson, Phys. Rev. A **39**, 3861 (1989).

[19] J. Fiol, C. Courbin, V.D. Rodriguez, and R.O. Barrachina, J. Phys. B **33**, 5343 (2000).

[20] C. Illescas, B. Pons, and A. Riera, Phys. Rev. A **65**, 030703 (2002).

[21] C. McGrath *et al.*, in *Abstracts of Contributed Papers of XXII-ICPEAC*, edited by S. Datz *et al.* (Rinton Press, Princeton, NJ, 2001).

[22] S. Suarez, C. Garbotti, G. Bernardi, P. Focke, and W. Meckbach, Phys. Rev. A **48**, 4339 (1993).

[23] M.B. Shah, D.S. Elliott, and H.B. Gilbody, J. Phys. B **20**, 3501 (1987).

[24] C.F. Kuyatt and J.A. Simpson, Rev. Sci. Instrum. **38**, 103 (1967).

[25] C. Illescas and A. Riera, Phys. Rev. A **60**, 4546 (1999).

[26] D.J.W. Hardie and R.E. Olson, J. Phys. B **16**, 1983 (1983).

[27] J.H. McGuire and L. Weaver, Phys. Rev. A **16**, 41 (1977).

[28] C. Illescas, B. Pons, and A. Riera, Phys. Rev. A **63**, 062722 (2001).

[29] C.O. Reinhold and J. Burgdorfer, J. Phys. B **26**, 3101 (1993).

[30] N. Stolterfoht, R.D. DuBois, and R.D. Rivarola, *Electron Emission in Heavy Ion-Atom Collisions* (Springer-Verlag, Berlin, 1997).

[31] B.S. Nesbitt, M.B. Shah, S.F.C. O'Rourke, C. McGrath, J. Geddes, and D.S.F. Crothers, J. Phys. B **33**, 637 (2000).